



OPEN ACCESS

EDITED BY Sue Chin Nang, Monash University, Australia

REVIEWED BY Joanna Marta Maiewska. University of Wrocław, Poland Renee Ng, University of Western Australia, Australia

*CORRESPONDENCE Hongyan Shi │
 │ hyshi@jlu.edu.cn

[†]These authors have contributed equally to this work and share first authorship

RECEIVED 09 April 2025 ACCEPTED 18 August 2025 PUBLISHED 12 September 2025

Zhang N, Li W, Du X, Daniyal D, Feng M-a, Xu J, Yang Z, Jiang H, Sheraz M, Huang H, Banerjee S and Shi H (2025) Identification and functional characterization of a novel Acinetobacter pittii bacteriophage-encoded depolymerase.

Front Cell Infect Microbiol 15:1608526 doi: 10.3389/fcimb.2025.1608526

© 2025 Zhang, Li, Du, Daniyal, Feng, Xu, Yang, Jiang, Sheraz, Huang, Banerjee and Shi. This is an open-access article distributed under the terms of the Creative Commons Attribution License (CC BY). The use, distribution or reproduction in other forums is permitted. provided the original author(s) and the copyright owner(s) are credited and that the original publication in this journal is cited, in accordance with accepted academic practice. No use, distribution or reproduction is permitted which does not comply with these terms.

Identification and functional characterization of a novel Acinetobacter pittii bacteriophage-encoded depolymerase

Na Zhang^{1,2†}, Wei Li^{3†}, Xue Du⁴, Danish Daniyal¹, Meng-ai Feng¹, Jiaoyang Xu¹, Zigin Yang¹, Hailin Jiang¹, Muhammad Sheraz¹, Honglan Huang¹, Santasree Banerjee⁵ and Hongyan Shi^{1*}

¹Department of Pathogen Biology, College of Basic Medical Sciences, Jilin University, Changchun, Jilin, China, ²Department of Genetics, Qujing Maternal and Child Health-care Hospital, Qujing, Yunnan, China, ³Department of Clinical Laboratory, The Third Bethune Hospital of Jilin University, Changchun, Jilin, China, ⁴Clinical Laboratory, Affiliated Hospital of Changchun University of Chinese Medicine, Changchun, China, ⁵Department of Genetics, College of Basic Medical Sciences, Jilin University, Changchun, China

Introduction: Acinetobacter pittii is increasingly recognized as a significant cause of nosocomial infections. Bacteriophage-encoded depolymerases that degrade capsular polysaccharides (CPS)—a major virulence factor of A. pittii—represent promising therapeutic tools.

Methods: This study identified and characterized a novel depolymerase, designated 31TSP, derived from the A. pittii bacteriophage 31Y. Its functional stability across various pH levels (5-11) and temperatures (4 °C to 121 °C) was assessed. The inhibitory effect of 31TSP on biofilm formation and its disruptive activity against preformed biofilms were evaluated using crystal violet staining, viable cell counts and scanning electron microscopy. Combinatorial treatments with 31TSP and ampicillin were conducted. Furthermore, the enzyme's stability under different ion concentrations (NaCl) and its ability to enhance serum bactericidal activity were tested under experimental conditions.

Results: Characterization demonstrated that 31TSP exhibits a broad host range against A. pittii, A. baumannii, and A. nosocomialis. The enzyme degraded the CPS of host bacteria and displayed inhibition effects on sensitive hosts. 31TSP retained functional stability across a wide pH range (5-11) and temperatures from 4 °C to 121 °C. Its inhibitory effect on biofilm formation and disruptive activity against preformed biofilms were confirmed. Notably, combinatorial treatment with 31TSP and ampicillin significantly enhanced biofilm inhibition and disruption at 24 hours post-treatment. However, 31TSP did not maintain stability under different ion concentrations (NaCl) and could not enhance serum bactericidal activity under the experimental conditions.

Discussion: These findings support the potential of 31TSP as an antibacterial agent against Acinetobacter infections. The observed synergy with conventional antibiotics, such as ampicillin, suggests a promising combinatorial strategy for

future therapeutics targeting *Acinetobacter*. The enzyme's stability under extreme conditions of temperature and pH further underscores its therapeutic potential. However, its instability in varying ionic environments and lack of serum bactericidal enhancement highlight aspects requiring further investigation for clinical application.

KEYWORDS

Acinetobacter pittii, bacteriophage, depolymerase, antibacterial activity, biofilm, antibiotic combination

1 Introduction

The Acinetobacter calcoaceticus-baumannii (ACB) complex has emerged as a significant nosocomial pathogen (Lee et al., 2021; Liu et al., 2015), causing diverse human infections including pneumonia, bacteremia, wound infections, meningitis, and urinary tract infections (Chusri et al., 2014). However, routine clinical diagnostics lack specificity for distinguishing ACB complex species (Vijayakumar et al., 2019). This limitation has historically led to underestimation of non-baumannii species in clinical settings (Pailhoriès et al., 2018).

Advances in molecular identification techniques (Teixeira et al., 2017; Marí-Almirall et al., 2019) and increased clinical isolation have established *A. pittii* as a prominent nosocomial pathogen (Chusri et al., 2014). Notably, carbapenem-resistant *A. pittii* (CRAP) strains have disseminated globally (Pailhoriès et al., 2018; Iimura et al., 2020; Tian et al., 2022), with rising antibiotic resistance rates (Zhu and Mathur, 2022). These trends necessitate urgent development of novel therapeutic agents against *A. pittii* infections.

Bacteriophages (phages) are natural co-evolutionary partners of bacteria, functioning as targeted antimicrobial agents through host-specific infection (Chen et al., 2022). However, their narrow host range—while advantageous for specificity—poses challenges for clinical implementation, necessitating precise strain-matched selection for therapeutic applications (Ringaci et al., 2022). Consequently, phage-derived enzymes (e.g., endolysins, depolymerases, and holins) have emerged as promising antibacterial candidates (Pires et al., 2016; Yuan et al., 2021).

Depolymerases are of particular interest due to their ability to degrade bacterial capsular polysaccharides (CPS), a major surface-exposed virulence factor. CPS serves as a protective barrier that facilitates bacterial adhesion, impedes antibiotic penetration, and confers resistance to phagocytosis and opsonization by host immune cells (Paczosa and Mecsas, 2016). CPS degradation sensitizes bacteria to immune-mediated clearance (Chen et al., 2022). Genes encoding depolymerases are typically situated near structural protein genes (e.g., tail fibers, tail sheath, baseplate, and neck connector proteins) in phage genomes and may occasionally share open reading frames (ORFs) with these genes (Cai et al., 2020). Bacteriophage-encoded depolymerases have been demonstrated to attenuate bacterial virulence in multiple

pathogens, including *Escherichia coli* (Chen et al., 2020), *Klebsiella pneumoniae* (Li et al., 2021; Cui et al., 2023), *A. baumannii* (Liu et al., 2019a), and *Proteus mirabilis* (Rice et al., 2021). However, research on depolymerase-mediated virulence reduction remains limited for *A. pittii* (Domingues et al, 2021). This gap underscores the need to identify and characterize additional depolymerases targeting *A. pittii* strains.

In this study, we identified an enzyme, TSP, capable of detaching *A. pittii* Ap31 CPS. We determined its activity under different pH values, temperatures, and ion concentrations. Additionally, we conducted research on the combined use of TSP and antibiotics against biofilms, as well as serum sensitivity assays mediated by TSP. Our findings indicate the applicability of bacteriophage-encoded capsule depolymerases as a novel strategy to control drug-resistant *A. pittii* infections.

2 Materials and methods

2.1 Acinetobacter pittii strain and the isolation of bacteriophage

All *Acinetobacter* strains employed in this study were isolated from the affiliated hospital of Changchun University of Chinese Medicine. Routine cultivation of these strains was conducted at 37 °C in LB broth or on LB agar (1.5% [wt/vol] agar).

Using A. pittii Ap31 as the host, bacteriophages were isolated from wastewater obtained from the First Hospital of Jilin University. Initially, the wastewater was centrifuged at 10,000 rpm for 10 minutes, and the supernatant was filtered through a 0.22 µm filter. The filtered supernatant was added to a 100 mL mixed bacterial culture in a logarithmic phase, and the mixture was incubated overnight at 160 rpm and 37 °C. The following day, the culture was centrifuged at 10,000 rpm for 10 minutes, and the supernatant was filtered through a 0.22 µm, 10 µL filter. A 10µL aliquot was then spotted onto LB plates overlaid with the corresponding bacterial strain to detect bacteriophage plaques. The bacteriophage was purified by repeating the double agar overlay method four times Bacteriophage titers were assessed using the double-layer agar method as described previously (Kropinski et al., 2009). The one step grow curve was tested

according to standard protocol for therapeutic phage preparation (Luong et al., 2020).

2.2 Observation of morphology through transmission electron microscopy

Bacteriophage particles were diluted 20 times, and 30 μ L of the diluted solution was dropped onto a 400-mesh copper grid. After adsorption for 15 minutes, the excess liquid was removed from the side. The sample was prepared for transmission electron microscopy (TEM). Negative staining was performed using 0.2% phosphotungstic acid for 30 seconds, excess liquid was removed, and the sample was air-dried for 1 hour. The specimen was then placed on the observation stage of the HT-7800 TEM (Hitachi, Japan) and bacteriophage morphology was observed and photographed under a voltage of 100 kV.

2.3 Preparation and sequencing analysis of bacteriophage genomes

As previously mentioned, bacteriophage genomic DNA was extracted using the phenol-chloroform method with slight modifications (Liu et al., 2013). Briefly, 500 μL of bacteriophage particles were treated at 37°C with a final concentration of 1 $\mu g/mL$ DNase I and RNase A for 1 hour to remove bacterial nucleic acids. Subsequently, 25 μL of 0.5 M EDTA (pH 8.0), 25 μL of 1 mg/mL proteinase K, and 20 μL of 10% SDS were added, followed by incubation at 56°C for 1 hour. After cooling to room temperature, bacteriophage genomic DNA was extracted using the phenol-chloroform method and then precipitated with ethanol. After thorough air-drying at room temperature, the precipitate was dissolved completely in 20-50 μL nuclease-free water and stored at -20°C.

The extracted bacteriophage genomic DNA was sent to Nanjing Parsona Genomics Technology Co., Ltd. for genome sequencing using the Illumina NovaSeq high-throughput sequencing platform. GeneMarkS software was employed for the analysis and prediction of open reading frames (ORFs) in the bacteriophage genome. HHpred (Söding et al., 2005) was used for remote protein homology detection and structure prediction of bacteriophage-encoded depolymerase ORFs. AlphaFold 2.0 (Jumper et al., 2021) was utilized for tertiary structure prediction with default settings, and PyMOL 2.5 was used for visualization.

2.4 Plasmid construction

Plasmid construction was performed using standard cloning methods. The ORF43 gene encoding the tail spike protein of bacteriophage 31Y, designated as 31TSP, was synthesized by Nanjing Parsona Genomics Technology Co., Ltd. It was then cloned into the pET28a plasmid using BamHI and HindIII restriction sites. The C-terminus of the protein was tagged with a 6×His tag.

2.5 Protein expression, purification, and identification

The constructed plasmid was transformed into Escherichia coli BL21 (DE3) cells. Recombinant plasmid-carrying E. coli BL21 cells were induced with 1 mM isopropyl-β-d-thiogalactopyranoside (IPTG) at 37 °C for 4 hours. Cells were harvested by centrifugation for subsequent protein purification. Ni-Berpharose FF (Beijing Borsodex Technology Co., Ltd.) was employed for nickel affinity chromatography to purify the enzyme. Briefly, the harvested cells were resuspended in sonication lysis buffer, and the cell suspension was lysed by sonication (20 minutes, 1 second/2 seconds). After centrifugation, the supernatant was collected. Then the supernatant was sequentially filtered through a 100 kDa 15 mL molecular weight cut-off (MWCO) centrifugal filter (Millipore) by centrifugation at $5,000 \times g$ for 8 min at 4 °C. The filtrate was collected and subsequently processed through a 20 kDa MWCO centrifugal filter (Millipore) under identical centrifugation conditions. Following centrifugation, proteins retained on the membrane were eluted. The eluted proteins were loaded onto Ni-Berpharose FF. The bound proteins were eluted with an imidazole gradient ranging from 10 to 500 mM. Proteins eluted with the imidazole gradient were collected, and the molecular weight of the depolymerase was assessed using sodium dodecyl sulfatepolyacrylamide gel electrophoresis (SDS-PAGE) (Chen et al., 2022). The concentration of the depolymerase was determined using the BCA Protein Assay Kit (Beyotime) (Walmagh et al., 2013).

Depolymerase activity was determined by spot assay (Hsieh et al., 2017). LB agar plates were inoculated with 200 μ L of fresh bacterial culture. After air-drying at room temperature, 5 μ L of purified depolymerase was spotted on the plates. Following overnight incubation at 37°C, the formation of translucent spots on the plates was observed. Based on the imidazole concentrations present in the various depolymerase concentration experiments, we examined the antibacterial effects of different concentrations of imidazole on *A. baumannii* using the same methodology.

Additionally, antibacterial activity of depolymerase 31TSP was assessed through viable cell counting. The depolymerase was added to logarithmic-phase host bacterial cultures at final concentrations of 100 $\mu g/mL$, 50 $\mu g/mL$, and 25 $\mu g/mL$. PBS of the same volume was added as a control. After incubation at 37 °C for 1, 2, 3, 4, 5, and 6 hours, each group was serially diluted tenfold, and viable cell counts were performed. The experiment was repeated three times, and the data were presented as bacterial reduction counts (control group - treatment group).

2.6 Determination of the host range of the phage and capsule depolymerase

A spot assay (Hsieh., et al. 2017) was conducted by observing 100 strains of Acinetobacter bacteria stored in the laboratory to ascertain the host range of Bacteriophage 31Y and Depolymerase 31TSP.

2.7 Quantitative assay of depolymerase activity

Depolymerase activity was quantitatively determined by measuring the release of reducing sugars during the reaction with 3,5-dinitrosalicylic acid (DNS). Initially, bacterial capsular polysaccharide (CPS) was extracted using the Bacterial Polysaccharide Extraction Kit (Solarbio, EX1750). Strain Ap31 was cultured on LB agar plates supplemented with 0.5% glucose at 37°C for 5 days. Cells were then scraped off with 2.5 mL of 0.9% (w/v) NaCl solution, and the harvested cells were used for CPS extraction according to the kit instructions (Oliveira et al., 2021). The freeze-dried CPS powder was re-suspended in PBS to a final concentration of 2 mg/mL and incubated with 100 µg/mL of 31TSP at 37°C for 1 hour, with PBS serving as control in place of CPS or 31TSP. DNS reagent (Solarbio, D7800) was added immediately at twice the volume in each reaction mixture, followed by a 5-minute reaction at 100°C. Absorbance was measured at 540 nm (Liu et al., 2019a). All experiments were independently conducted three times.

2.8 Hemolysis assay

The impact of 31TSP on human red blood cell (RBC) hemolysis was assessed using a modified version of a previously described method (Chen et al., 2022). Isolated RBCs were washed twice with PBS (2,000 rpm, 10 min), diluted in PBS to a 5% (v/v) concentration, and then incubated with 31TSP at 37°C for 1 hour, with PBS and 0.1% Triton X-100-treated RBCs serving as negative and positive controls, respectively. After centrifugation at 8,000 rpm for 10 min, 100 μL of the supernatant was transferred to a 96-well microplate, and 100 μL of PBS was added to each well, °Cresulting in a final volume of 200 μL . Hemoglobin levels were measured at 540 nm. All experiments were independently conducted three times.

2.9 Cytotoxicity analysis of 31TSP

HEK293 cells (human embryonic kidney cells) were cultured in DMEM (Gibco) supplemented with 10% FBS (HyClone) at 37°C under 5% CO₂ and 90% humidity for 2 days. Subsequently, the cells were trypsinized and seeded into 96-well plates at a density of 10^4 cells per well and incubated at 37°C for 24 h. Then, the medium was replaced by 200 μ L new medium containing 31TSP (50 μ g/mL). After 12 h incubation, 10 μ L WST-8 solutions were added into each well for another 2 h incubation at 37°C. The cell viability was evaluated by absorbance at 450 nm using a microplate reader (Tecan). Three independent experimental repeats were performed, each with triplicate wells per group including PBS controls.

2.10 Depolymerase stability analysis

Stability analysis of the depolymerase was conducted following a modified version of the method described in a previous study (Oliveira et al., 2019). To evaluate the pH stability of 31TSP, phosphate-buffered saline (PBS) solutions were adjusted to pH values ranging from 1 to 14 using HCl or NaOH. For each pH condition, 31TSP (final concentration: 100 $\mu g/mL$) and 100 μL of log-phase bacterial culture were added into 1.8 mL of the corresponding PBS. The total reaction volume was adjusted to 2 mL using PBS at the same pH. Control groups contained only PBS (at respective pH values) and an equivalent volume of bacterial suspension. All samples were incubated at 37°C with shaking for 3 h. After incubation, serial dilutions were performed, followed by overnight plating for colony counting. The antimicrobial activity of 31TSP at different pH levels was determined by calculating the reduction in bacterial counts (CFU/mL) relative to the corresponding pH-matched control (Δlog reduction). A higher reduction value indicates greater enzymatic stability and activity under the tested pH conditions.

For temperature stability, 31TSP was respectively treated at temperatures of 4, 25, 37, 50, 60, 70, 80, 90, 100, and 121°C for 30 minutes. After cooling to room temperature, 31TSP was mixed with the host bacterial culture to achieve a final concentration of 100 $\mu g/$ mL. Same volume of PBS was added into bacteria culture as control. All samples were incubated at 37°C with shaking for 3 h. Then the living bacteria were cultured and counted as in pH stability test.

To assess the effect of ionic strength on 31TSP activity, log-phase bacterial culture was mixed with 31TSP at a final concentration of 100 $\mu g/mL$. The ion concentration of the mixture was then adjusted by adding 1 M NaCl to achieve final NaCl concentrations of 50 $\mu M,~150~\mu M,~300~\mu M,~and~500~\mu M.$ Negative control was prepared by adding an equivalent volume of sterile distilled water (ddH₂O) instead of NaCl (0 μM). All samples were incubated at 37°C with shaking for 3 h. Then the living bacteria were cultured and counted as in pH stability test.

2.11 Serum killing assay

The optimal volume ratio of serum to enzyme-treated bacteria was determined as described previously (Liu et al., 2019b). Overnight cultured host bacteria were co-incubated with or without 100 $\mu g/mL$ TSP at 37 °C for 3 hours. The enzyme-treated host bacteria were added to healthy human serum at volume ratios of 3:1, 1:1, or 1:3, with a final reaction volume of 200 μL . After incubation at 37 °C for 3 hours, bacterial viability was determined by colony counting. The experiment was independently conducted three times.

To assess the role of serum complement in the serum bactericidal assay, a strain sensitive to Bacteriophage 31Y and 31TSP (*A. pittii* Ap30) and a strain insensitive (*A. baumannii* Ab5) to 31Y and 31TSP were also selected (Chen et al., 2022). Bacteria were treated with enzyme for 3 hours at 37°C and then mixed with active or heat-inactivated serum (56°C, 30 minutes) at a 3:1 volume ratio. After incubation at 37°C for 3 hours, bacterial viability was determined by colony counting. Untreated bacteria, along with equal volumes of PBS, 31TSP, active and heat-inactivated serum, were cultured as controls, and bacterial

viability was determined after 6 hours of incubation at 37°C. All experiments were independently conducted three times.

2.12 Biofilm inhibition assay

As previously described, we investigated the inhibitory effects of 31TSP and antibiotics on biofilm, with slight modifications (Chen et al., 2022). The host bacterium Ap31 was cultured to the logarithmic phase, treated with 0.1M PBS (control group), 31TSP (100 µg/mL), ampicillin (16 µg/mL, MIC), or their combination (31TSP + ampicillin) at a final volume of 100 µL/well in a 96-well plate, and incubated at 37°C for 3h, 6h, 9h, 12h, and 24h, respectively. After incubation, all culture media were removed, and the wells were washed three times with 100 µL of 0.1M PBS. The plate was air-dried at room temperature, stained with 100 µL of 0.1% (w/v) crystal violet for 10 min, and then destained with 100 μL of 95% ethanol for 10 min. The remaining biofilm biomass was quantitatively measured at 570 nm wavelength using a microplate reader (BioTek). The anti-biofilm activity was assessed by counting planktonic live bacteria (Wilson et al., 2017). All experiments were independently conducted three times.

2.13 Biofilm removal assay

The host bacterium Ap31 was cultured to the logarithmic phase and dispensed into a 96-well plate at 100 µL/well. Based on the growth matrix curve of the host bacterium (Supplementary Figure 1), the maximum biofilm biomass formation was determined at 9h, and the plate was incubated at 37°C for 9h. The biofilm was washed twice with 0.1M PBS and then treated with 0.1M PBS (control), 31TSP (100 µg/mL), ampicillin (16 µg/mL, MIC), or their combination (31TSP + ampicillin) at a final volume of 100 µL/well, followed by incubation at 37°C for 3h. At the end of the incubation period, quantification of the remaining biomass was performed using crystal violet as described in the inhibition assay (Chen et al., 2022). Additionally, the anti-biofilm activity was assessed by counting live bacteria within the biofilm (Wilson et al., 2017). After treating the biofilm as described above, wells were washed three times with 0.1M PBS. Subsequently, a pipette device was used to thoroughly mix wells containing the biofilm, converting biofilm cells into planktonic cells. Each sample was serially diluted and subjected to live bacterial counting. All experiments were independently conducted three times.

2.14 Scanning electron microscopy observation

Detection of the Impact of 31TSP and Antibiotics on Biofilm Formation and Eradication in *A. pittii*: (1) Biofilm Inhibition Observation: High-pressure sterilized cover slips were placed in a 24-well plate. The host bacterium at the logarithmic phase was treated with 0.1M PBS (control), 31TSP (100 µg/mL), ampicillin (16 µg/mL,

MIC), or their combination (31TSP + ampicillin) at a final volume of 1 mL/well. The mixtures were cultured at 37 °C until 9h (maximum biofilm biomass formation). After incubation, all mixtures were removed, and the coverslips were washed three times with 1 mL of 0.1M PBS. Samples treated with depolymerase for varying durations were arranged in reverse chronological order (longest to shortest treatment time) according to the scheduled electron microscopy time slot. The coverlips from all treatment groups were harvested simultaneously and processed for electron microscopy observation. The coverslips were air-dried at room temperature and subjected to gold coating. The impact of 31TSP and antibiotics on biofilm formation in A. pittii was observed using a scanning electron microscope (JSM-7900F). (2) Biofilm Eradication Observation: High-pressure sterilized coverslips were placed in a 24-well plate. The host bacterium at the logarithmic phase was dispensed into each well at 1 mL/well and cultured at 37 °C until 9h. After washing twice with 0.1M PBS, the coverslips were treated with 0.1M PBS (control), 31TSP (100 $\mu g/mL$), ampicillin (16 $\mu g/mL$, MIC), or their combination (31TSP + ampicillin) at a final volume of 1 mL/well. The mixtures were incubated at 37 °C for 3h. After incubation, all mixtures were removed, and the coverslips were washed three times with 1 mL of 0.1M PBS. The coverslips were air-dried at room temperature and subjected to gold coating. The impact of 31TSP and antibiotics on biofilm eradication in A. pittii was observed using a scanning electron microscope (JSM-7900F).

2.15 Statistical analysis

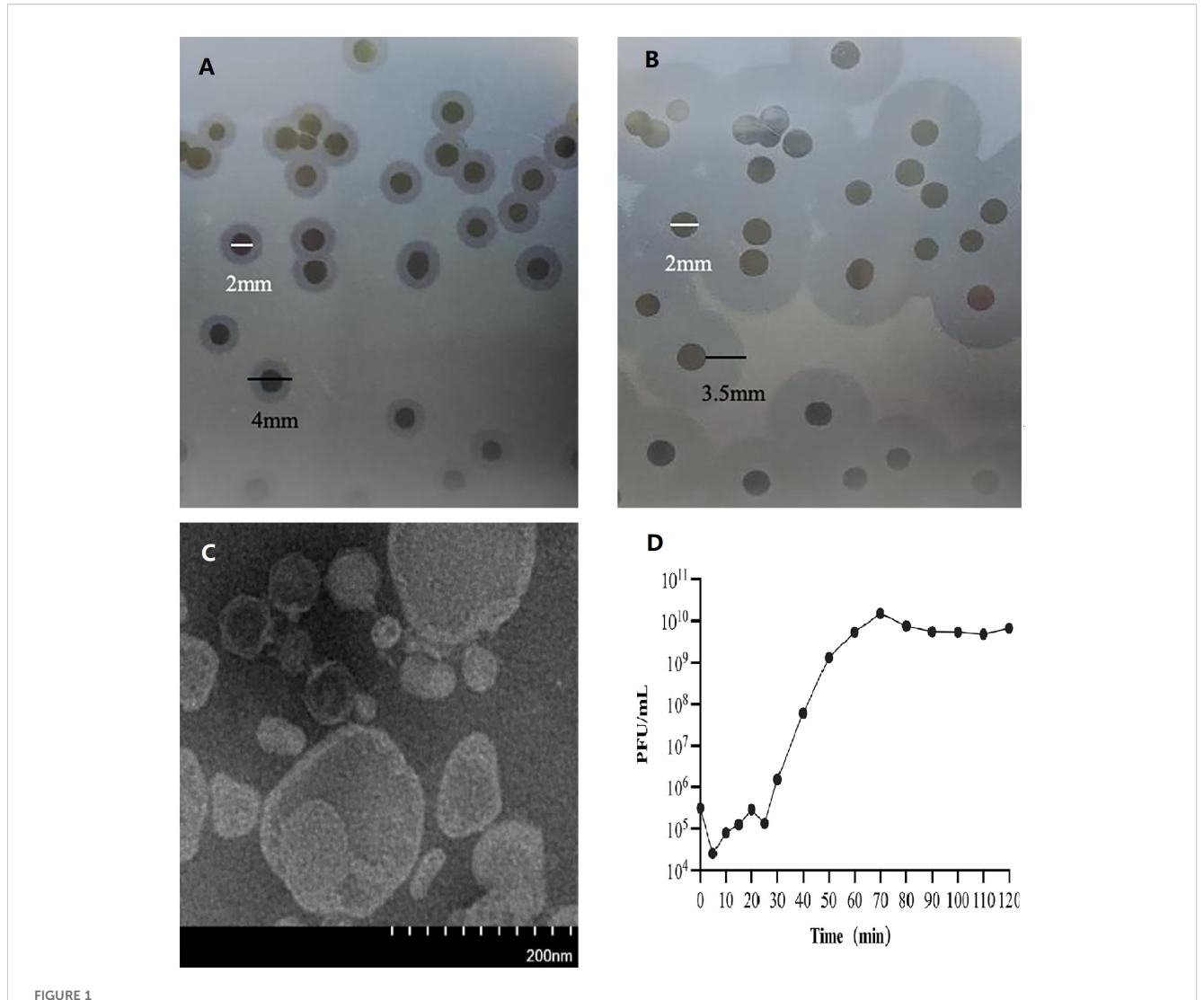
All data represent the average of three independent experiments, and the results are expressed as the mean \pm standard deviation. Statistical significance was analyzed using SPSS Statistics 25.0 software, with p < 0.05 considered statistically significant. Graphs were created using Prism 7.

3 Results

3.1 Morphology and one-step growth curve of phage

When the isolated was inoculated onto a double-layer agar plate containing the host bacterium Ap31 (antibiotic resistance spectrum detailed in Supplementary Table 1), transparent plaques surrounded by a semi-transparent halo were formed (diameter approximately 2.5 mm) (Figures 1A, B). As the cultivation time increased, the halo area gradually enlarged, with the diameter expanding from approximately 4 mm (cultivation for 7 hours) to about 9 mm (cultivation for 20 hours). Transmission electron microscopy images revealed that the bacteriophage 31Y had an icosahedral head (diameter of about 60 nm) and a non-contractile short tail (about 15 nm) (1C).

After propagation, concentration, and purification, the final titter of bacteriophage 31Y was determined to be 2×10^{10} PFU/mL. Infection of the Ap31 strain with bacteriophage 31Y at a multiplicity



Transparent plaques and halos produced by bacteriophage 31Y. (A) Transparent plaques and halos were observed after 7 hours of cultivation. (B)Transparent plaques and halos were observed after 20 hours of cultivation. A semi-transparent halo expanded with prolonged incubation time. (C) Transmission electron micrograph of bacteriophage 31Y. (D) One-step growth curve of bacteriophage 31Y.

of infection (MOI) of 0.001 was conducted for a one-step growth curve analysis. As shown in Figure 1D, the latent period of bacteriophage 31Y was approximately 25 minutes, the burst period was 45 minutes, and it reached stability after 70 minutes. The burst size of bacteriophage 31Y was approximately 48 PFU/cell.

3.2 Whole genome sequencing analysis and structural analysis of depolymerase

The whole genome sequencing results revealed that the size of bacteriophage 31Y genome was 41, 254 bp, arranged as a linear double-stranded genome with a G+C content of 39.26%. The nucleotide composition was 31.15% A, 17.13% C, 22.14% G, and 29.58% T. The annotated genomic sequence reregistration number for bacteriophage 31Y is currently pending and will be provided upon final registration, the sequence is available as supplementary data.

Gene prediction using the GeneMarkS tool identified 49 open reading frames (ORFs) within the bacteriophage 31Y genome, covering 37,992 bp with an average length of 775.35 bp. The accession number of bacteriophage 31Y genome in NCBI is PV467367 (*Acinetobacter* phage A31Y, complete genome - Nucleotide - NCBI). According to BlastN analysis and the document of International Committee on Taxonomy of Viruses, Acinetobacter phage A31Y belongs to *Autographiviriles, Autoscriptoviridae*.

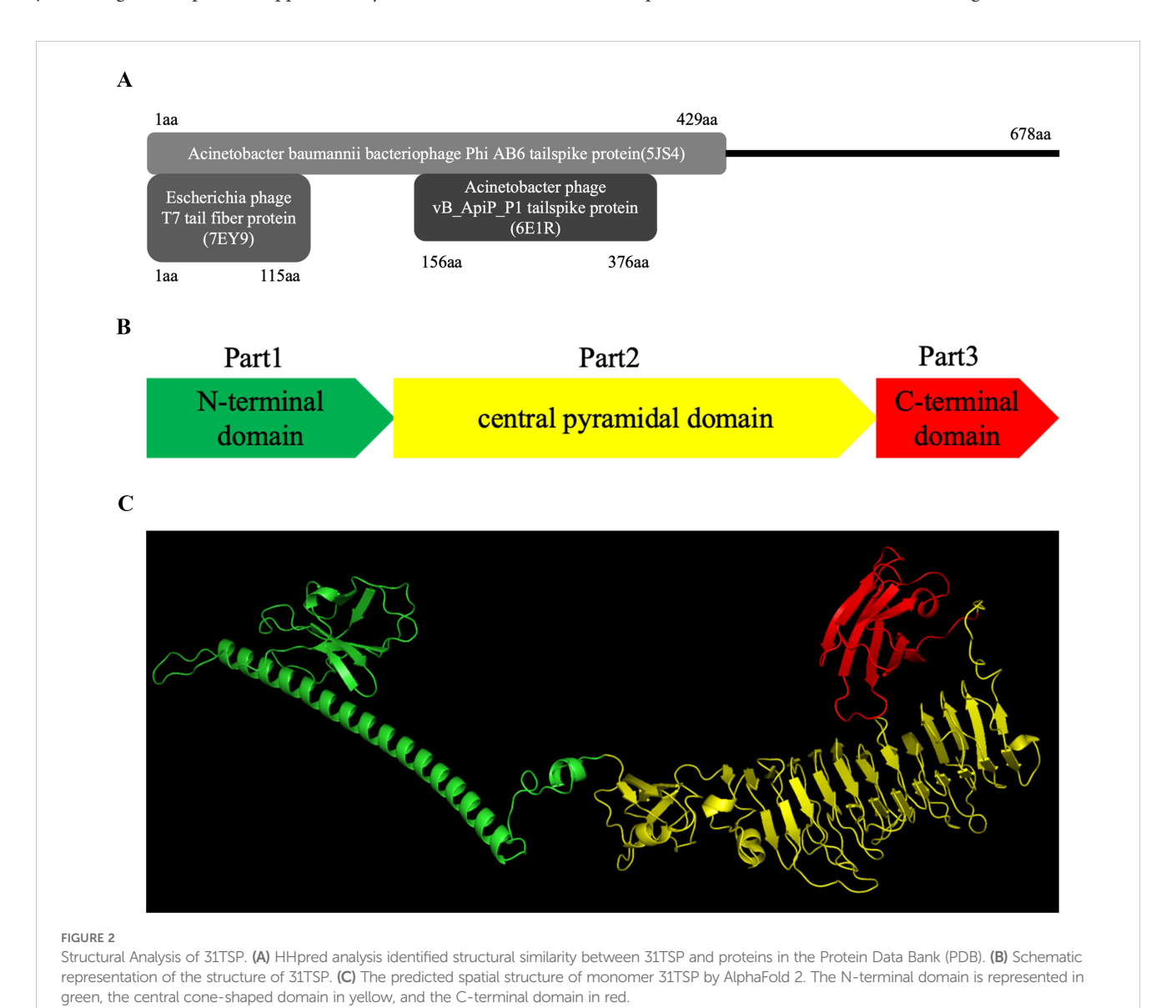
Among these ORFs, ORF43 with a size of 678 amino acids, was identified as the gene encoding the tail spike protein as it showed high homology with tail spike proteins of several Acinetobacter phages, such as *Acinetobacter* phages Paty (QQM15083), *Acinetobacter* phage vB_AbaP_ABW311 (CAL1776920) and *Acinetobacter* phage Pipo (QQO92973). These proteins are classified as structural depolymerases originating from these bacteriophages. Although no conserved domains could be found by NCBI Conserved Domain Search, HHpred analysis indicated

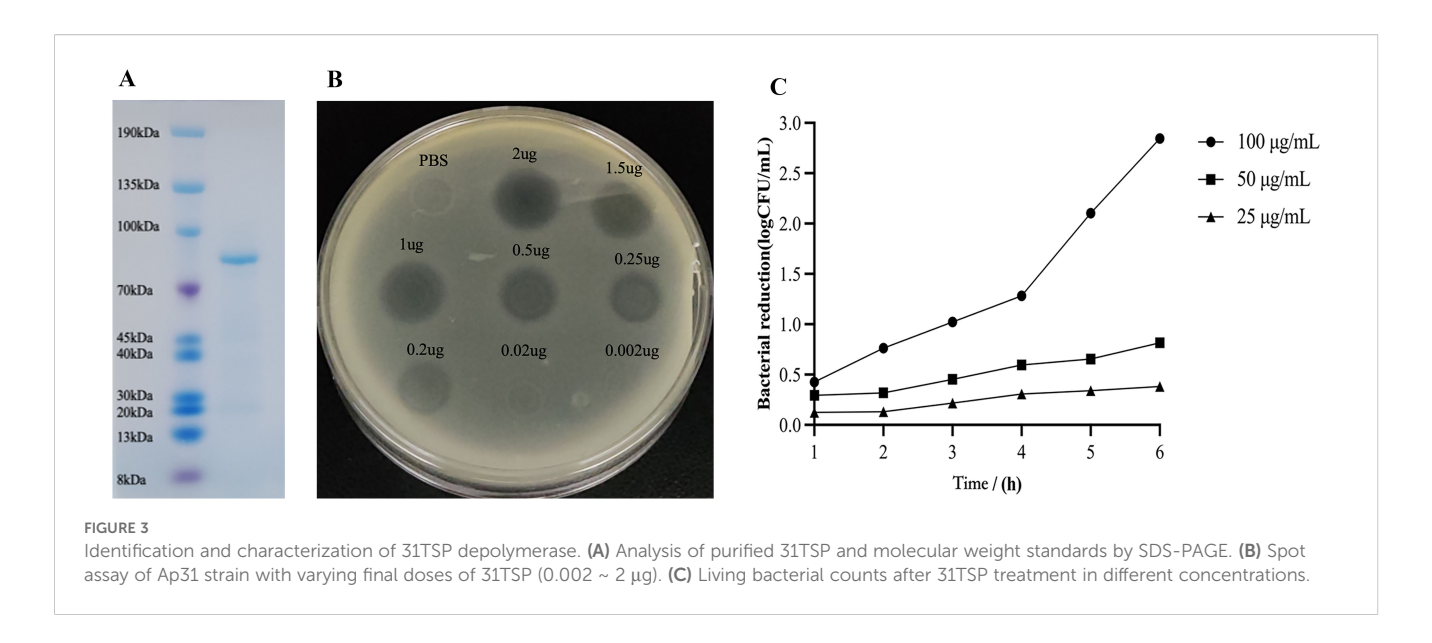
high structural similarity between the N-terminal region of 31TSP to the N-terminal region of tail fiber/spike protein of the T7 phage (Garcia-Doval and van Raaij, 2012) and *A. baumannii* bacteriophage AB6 (Figure 2A).

The predicted structure of the monomer of the depolymerase encoded by bacteriophage 31Y, as determined by AlphaFold 2, revealed three distinct domains (Figures 2B, C). The first part exhibited an N-terminal domain with an antiparallel β -sheet structure followed by α -helices, responsible for the attachment of these proteins to the bacteriophage particles, playing a role in the initial interaction with the bacterial host (Drobiazko et al., 2022). The second part constituted a cone-shaped interlocking pyramid domain mainly composed of parallel short β structures, commonly involved in host recognition and exhibiting depolymerase activity (Garcia-Doval and van Raaij, 2012). The simulated third part represented the C-terminal domain, consisting of an antiparallel β -sheet region composed of approximately 100 amino acids.

3.3 Expression, purification, and identification of depolymerase

The gene ORF43, encoding the tail spike protein, was cloned into an expression vector and purified through Ni-NTA affinity chromatography, yielding a recombinant product at 223 μ g/mL concentration. SDS-PAGE analysis confirmed the presence of a recombinant protein, 31TSP, with an approximate molecular weight of 75 kDa (Figure 3A). As the total number of amino acids in the protein sequence was 678, the purified protein band observed on the gel corresponds to a depolymerase monomer. To validate the enzyme's activity post-purification, a plaque assay was conducted. For every test, 5 μ L depolymerase in different concentration were dropped on bacteria lawn. The results demonstrated that purified 31TSP formed a semi-transparent halo on the lawn of host strain Ap31 (Figure 3B). The area of the semi-transparent halo decreased with decreasing concentrations of





31TSP, disappearing when the total amount of the enzyme spotted onto the bacterial lawn was reduced to 0.02 μg (4 $\mu g/mL$). Antibacterial activity experiments indicated a proportional relationship between 31TSP concentration and antibacterial efficacy. The most significant reduction in bacterial count was observed at a concentration of 100 $\mu g/mL$ (Figure 3C). Thus, 31TSP exhibited robust depolymerase activity. However, the group treated with imidazole at the same concentration as the experimental groups showed no antibacterial effect. Please refer to Supplementary Figure 1 for the results.

3.4 Host range of bacteriophage and depolymerase

The depolymerizing capability of 31TSP and the host range of bacteriophage 31Y were assessed using a collection of 98 strains of *Acinetobacter* stored in our laboratory (Supplementary Table 2). Overall, among these *Acinetobacter* strains 38 (38/98, 38.8%) were susceptible to depolymerization by 31TSP, while only 5 (5/98, 5.1%) strains were susceptible to lysis by bacteriophage 31Y. Notably, all 5 strains susceptible to bacteriophage 31Y belonged to *A. pittii*. In contrast, among the 38 strains susceptible to 31TSP depolymerization, aside from the 5 A. *pittii* strains lysed by bacteriophage 31Y, an additional 1 A. *pittii*, 1 A. *nosocomialis*, and 31 A. *baumannii* strains were susceptible, significantly having a broader host range than bacteriophage 31Y.

3.5 Quantification of depolymerase activity

The activity of 31TSP was quantified by measuring the release of reducing sugars from bacterial surface polysaccharides. The OD₅₄₀ values for CPS and 31TSP in PBS were 0.064 \pm 0.005 and 0.105 \pm 0.002, respectively. In contrast, the OD₅₄₀ for CPS treated with 31TSP was 0.157 \pm 0.002 (Figure 4A). The increase in OD₅₄₀ for

31TSP-treated CPS indicates the production of reducing sugars, suggesting that surface polysaccharides extracted from the host bacteria were degraded by the depolymerase.

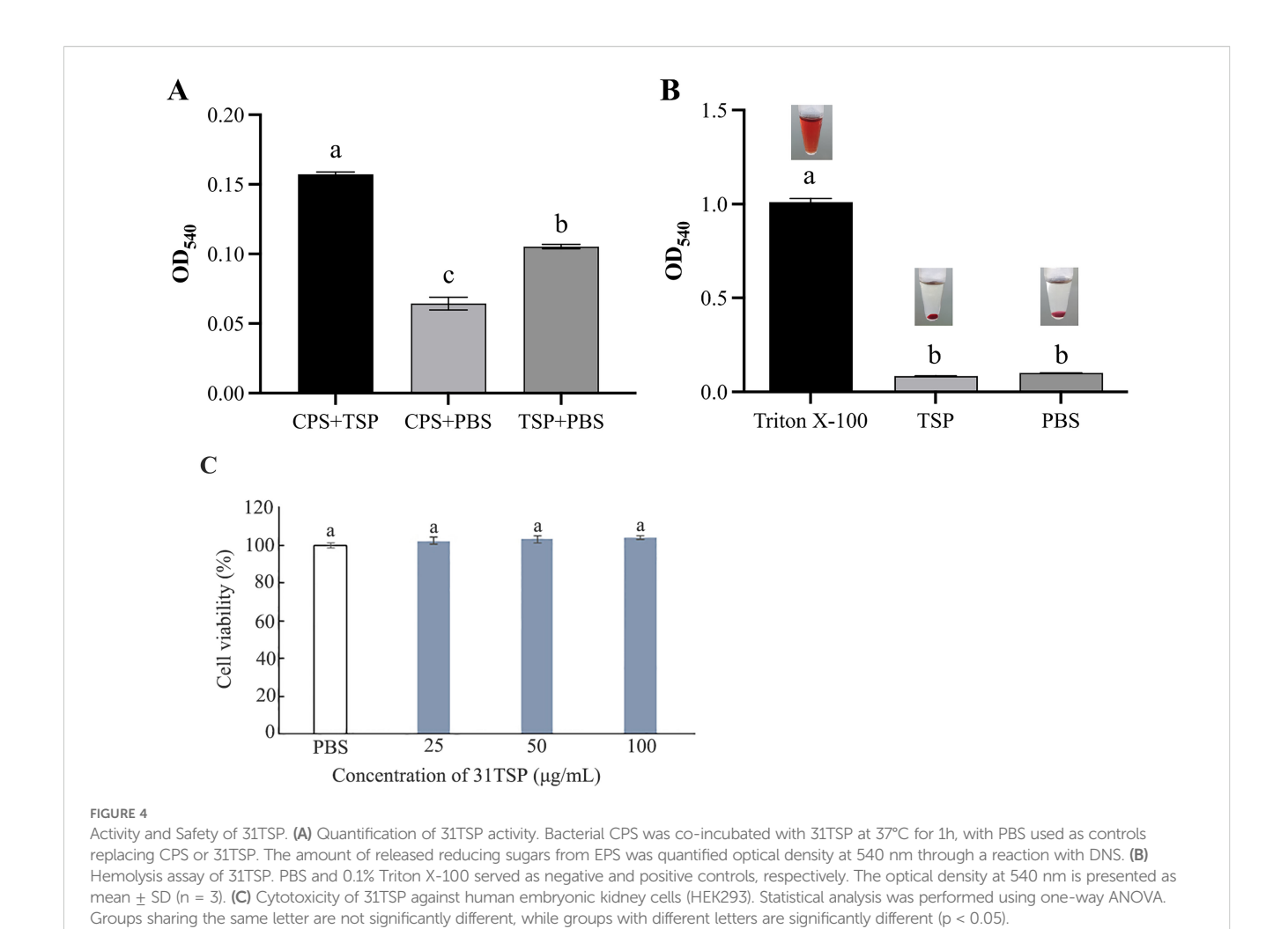
3.6 Hemolysis assay and cytotoxicity analysis

Human blood cells and human embryonic kidney cells (HEK293) were used to evaluate the toxicity of 31TSP to mammalian cells. The results of the hemolysis assay (Figure 4B) showed no significant difference between 31TSP and the negative control group (PBS group) after 1 hour of incubation with red blood cells, and no hemolysis was observed. Figure 4C showed 31TSP has no cytotoxicity against HEK293. These results suggest 31TSP may be a safe therapeutic approach.

3.7 Stability of depolymerase

The activity of 31TSP was assessed under various environmental conditions, including temperature, pH, and ion strength (Figure 5). Encouragingly, the enzyme demonstrated remarkable temperature stability, maintaining high activity after 30 minutes of treatment across a range of 4 °C to 121 °C (Figures 5A, B). The maximum reduction in viable bacterial count occurred at 37 °C, reaching 3.104 \pm 0.016 log, indicating the highest activity. Even after treatment at 100 °C and 121 °C for 30 minutes, the enzyme still caused reductions of 1.484 \pm 0.055 and 1.762 \pm 0.053 log, respectively. Furthermore, the enzyme remained active over a broad pH range from 5 to 11 (Figure 5C), and even at pH 4 some depolymerase keep weak activity.

Ion concentration significantly decreased the activity of 31TSP, with a notable impact even at 50 mM ion concentration, resulting in a reduction of 0.525 \pm 0.050 log compared to the control group (Figure 5D). The influence of ion concentration on depolymerase activity appeared unrelated to a dose-dependent effect.



3.8 The effect of depolymerase on serum bactericidal activity

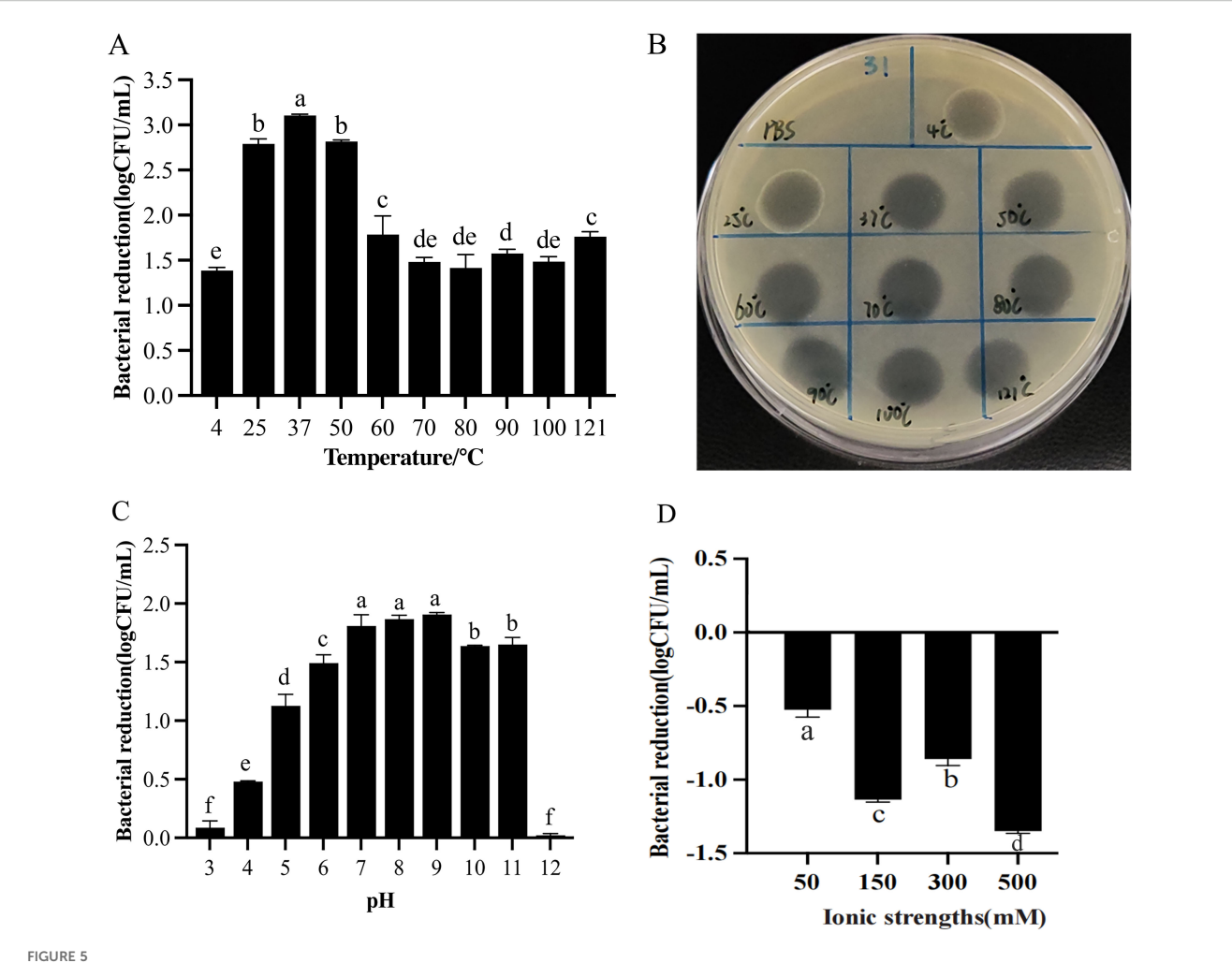
Compared to 31TSP untreated bacteria, the number of host bacteria (Ap31) treated with 31TSP decreased when mixed with varying volumes of serum (P < 0.05), but the differences were not observed among different serum proportion groups (Figure 6A). In subsequent experiments, a serum proportion of 25% was used.

To assess the role of serum, we chose $A.\ pittii$ Ap30, Ap31 and $A.\ baumannii$ Ab5, as the target bacteria. Ap31 and Ap30 are sensitive to phage 31Y and 31TSP, but Ab5, is insensitive to phage 31Y and 31TSP. These three test strains exhibited resistance to serum killing, continuing to grow in human serum in the absence of 31TSP. Conversely, after treatment with 31TSP and subsequent incubation with active serum or inactive serum for 3 hours, the bacterial count of host strain Ap31 and Ap30 are higher than TSP treated groups (P < 0.05). While the insensitive strain Ab5, all experimental groups exhibited almost no reduction in bacterial count than PBS control (Figure 6B). Therefore, the experimental *Acinetobacter* strains are resistant to serum killing, and serum and inactivated serum showed inhibitory effect on 31TSP.

3.9 Anti-biofilm activity

We first evaluated the inhibitory effects of 31TSP on biofilm formation using crystal violet staining. Quantitative analysis demonstrated that while ampicillin alone (16 μ g/mL, MIC) showed partial inhibition of biofilm formation compared to PBS controls at both 6 and 24 hours (p < 0.05), 31TSP alone exhibited significantly stronger inhibitory effects (p < 0.05). The combination of 31TSP and ampicillin showed the most pronounced biofilm inhibition, particularly at the 24-hour time point (Figure 7A). However, at earlier points (6 hours), no significant difference in biofilm inhibition was observed between 31TSP alone and the combination treatment (p > 0.05).

Viable cell counting results demonstrated that, with prolonged incubation time, the planktonic bacterial count in the PBS control group tended to stabilize. In comparison to the PBS control group, the exclusive use of 31TSP resulted in a reduction of planktonic bacterial counts by 1.280, 2.825, 3.940, 1.306, and 0.675 log at 3, 6, 9, 12, and 24 hours, respectively. Furthermore, the combination with ampicillin further enhanced this inhibitory effect, leading to reductions of 0.027, 0.964, 1.360, 3.319, and 2.379 log at the



Stability of 31TSP. (A) Effect of temperature on 31TSP activity. (B) Spot test of 31TSP against Ap31 strain under different temperature treatment conditions. (C) Effect of pH on 31TSP activity. (D) Effect of ion concentration on 31TSP activity. The values are presented as the log reduction in bacterial count (means \pm SD; n = 3), and the statistical analysis was assayed by one-way ANOVA. Groups sharing the same letter are not significantly different, while groups with different letters are significantly different (p < 0.05).

respective time points (Figure 7B). Although the inhibitory effect of sole 31TSP application on planktonic bacterial growth diminished significantly at 12 and 24 hours, the combined treatment with ampicillin effectively suppressed planktonic bacterial growth. SEM further validated the results (Figure 7C). Our findings unequivocally confirm the efficacy of both sole 31TSP application and its combination with ampicillin in preventing *A. pittii* biofilm formation.

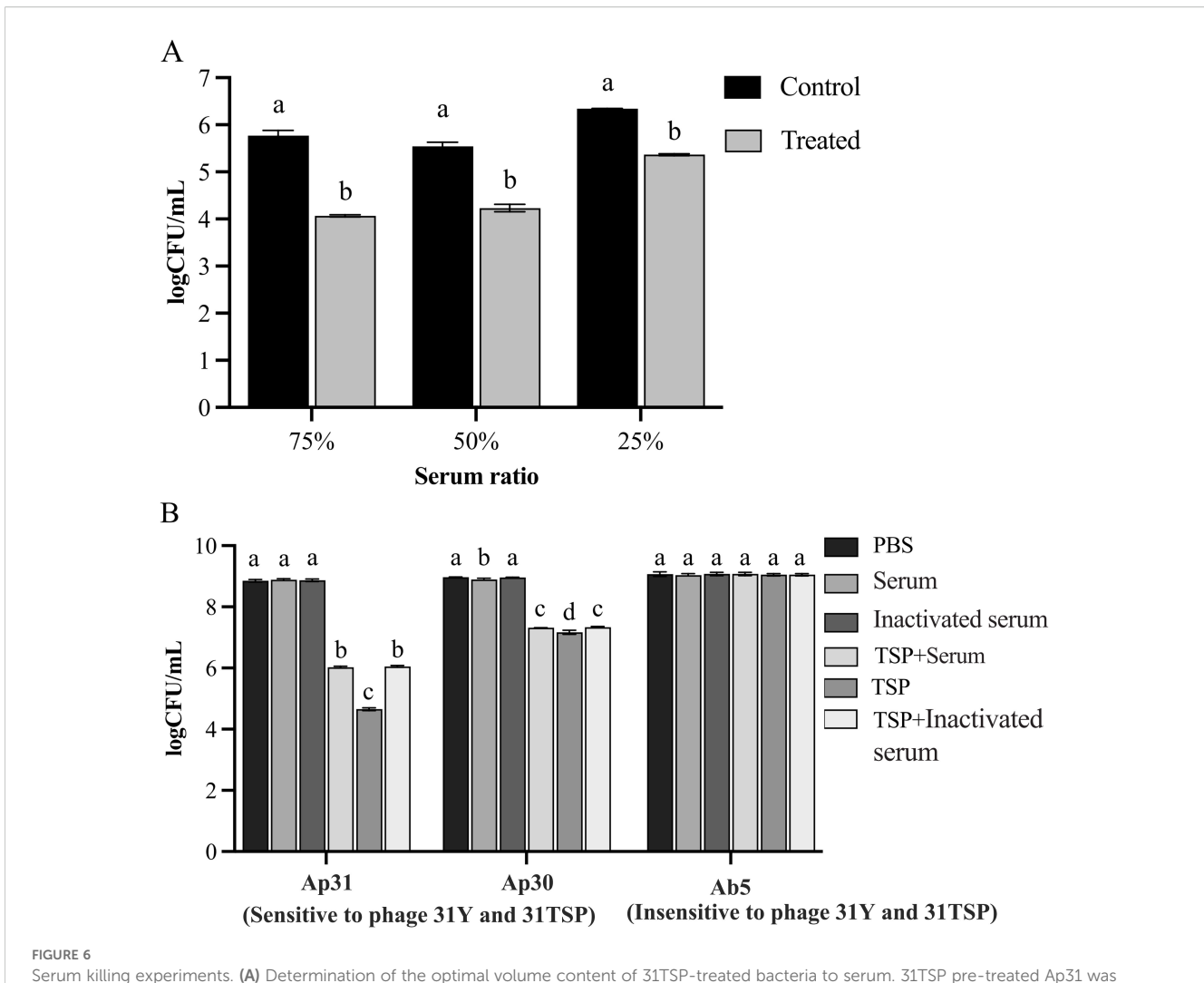
Subsequently, we assessed whether 31TSP alone or in combination with ampicillin could disrupt pre-formed biofilms. Crystal violet staining results indicated that, compared to the PBS control group, the sole administration of ampicillin failed to disrupt pre-formed biofilms. In contrast, the exclusive use of 31TSP and its combination with ampicillin effectively disrupted the pre-formed biofilms (p < 0.05). However, there were no significant differences between the sole use of 31TSP and its combination with ampicillin (p > 0.05) (Figure 8A).

Based on viable cell counting results, sole treatment with 31TSP could disrupt the host bacteria, reducing the residual host bacteria

by 3.104 log compared to the PBS control group. The combination treatment further decreased the remaining host bacteria by 0.095 log, with no significant differences observed between the sole use of 31TSP and its combination with ampicillin (p > 0.05). In the absence of 31TSP, ampicillin exhibited inefficient killing of bacteria embedded in the biofilm, resulting in a modest reduction of 0.095 log (Figure 8B). SEM observations were consistent with the aforementioned results (Figure 8C). These data suggest that 31TSP can effectively eradicate pre-formed biofilms and enhance the antibiofilm activity of ampicillin.

4 Discussion

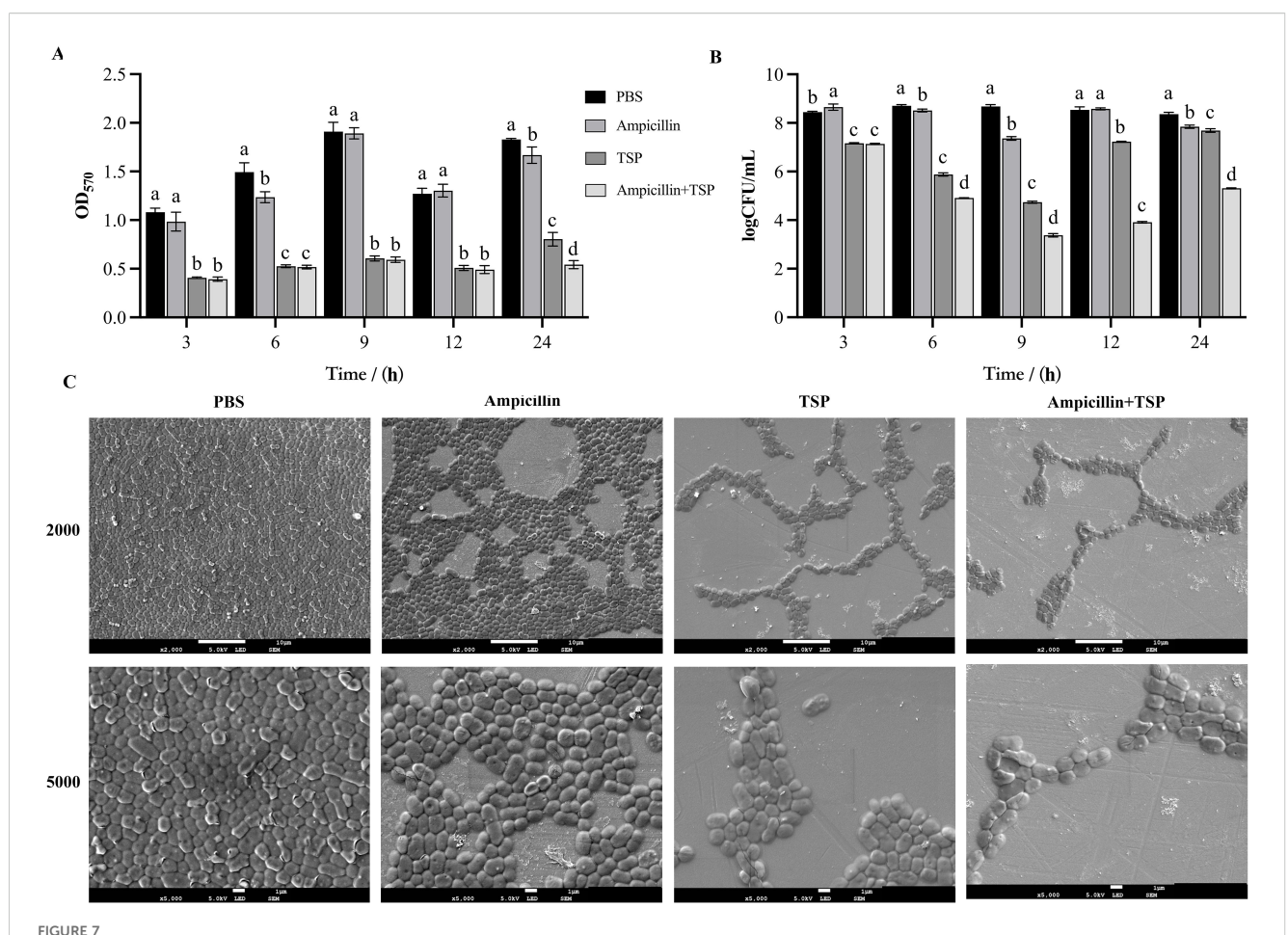
A. pittii, as a member of the ACB complex, often faces misidentification due to its phenotypic similarity to A. baumannii, exacerbated by technical limitations in clinical laboratory identification methods (Pailhoriès et al., 2018; Molina et al., 2010; Chen et al., 2018). However, with an increasing number



Serum killing experiments. (A) Determination of the optimal volume content of 31TSP-treated bacteria to serum. 31TSP pre-treated Ap31 was incubated with human serum at a volume ratio of 3:1, 1:1 or 1:3 for 3 hours and viable bacteria were counted. (B) A. pittii Ap30 and A. pitti Ap31are sensitive to 31TSP and bacteriophage 31Y, A. baumannii Ab5 was insensitive to 31TSP and bacteriophage 31Y. These strains were used as target bacteria to test the combination of 31TSP with serum or inactivated serum. 31TSP-treated bacteria were incubated with serum or inactivated serum at a 3:1 volume content. Then the living bacteria were cultured and counted. Data is expressed as mean \pm SD (n = 3), and statistical analysis was performed by one-way ANOVA. Groups sharing the same letter are not significantly different, while groups with different letters are significantly different (p < 0.05).

of clinical isolates and advancements in molecular identification techniques (Teixeira et al., 2017; Marí-Almirall et al., 2019; La Scola et al., 2006), the relevance of the A. pittii species is growing. A research report from a French hospital indicates that A. pittii is more frequently isolated from blood cultures compared to A. baumannii, underscoring its clinical significance (Pailhoriès et al., 2018). Studies also suggest a 17% mortality rate within 28 days for A. pittii-induced bacteremia (Liu et al., 2017). Recent multicenter surveys in Japan reveal A. pittii as the most common species causing invasive Acinetobacter infections (Kiyasu et al., 2020). Moreover, in vitro and in vivo models highlight the higher pathogenicity of A. seifertii and A. pittii compared to A. baumannii and A. nosocomialis (Cosgaya et al., 2019; Kuo et al., 2013). With increasing attention on A. pittii, cases of A. pittii carrying carbapenemase NDM-1 have been frequently reported, contributing to increased carbapenem resistance and alterations in resistance mechanisms (Bogaerts et al., 2013; Chen et al., 2019; Pailhoriès et al., 2017). A recent study reported a severe pneumonia case associated with a pan-drug-resistant *A. pittii* infection in a patient with chronic obstructive pulmonary disease three years post-double lung transplant (Yang et al., 2021).

In response to the growing resistance of *A. pittii*, this study investigates the potential of bacteriophage-encoded depolymerases as a novel therapeutic strategy. Understanding of the pathogenic mechanisms of *A. pittii* is currently limited. However, it is known that *A. pittii* possesses a thick capsular polysaccharide (CPS) layer surrounding its cells, considered a crucial virulence factor, hindering the penetration of certain peptide antibiotics and shielding the bacterium from host immune system attacks (Drobiazko et al., 2022). Importantly, bacteriophage-encoded depolymerases have the capability to degrade bacterial CPS, rendering the bacteria more susceptible to host immune system



Inhibition of Biofilm Formation by 31TSP and Ampicillin. (A) Crystal violet staining of biofilms. (B) Living planktonic bacterial counting assay. (C) Scanning electron microscopy observation at 24 hours. Ap31 bacterial cultures were treated with PBS (control group), 31TSP (100 μ g/mL), ampicillin (16 μ g/mL, MIC), or their combination (31TSP + ampicillin), followed by crystal violet staining, planktonic bacterial counting, and scanning electron microscopy observation. Data are presented as mean \pm SD (n = 3), and statistical analysis was conducted using one-way ANOVA. Different letters (a-c) indicate significant differences (p < 0.05).

mediated killing (Chen et al., 2022; Liu et al., 2020; Majkowska-Skrobek et al., 2018).

According to HHpred analysis, the depolymerase 31TSP exhibits structural similarity to tail spikes from various bacteriophages. Its N-terminal portion shares a structural resemblance with the N-terminal segment of the T7 bacteriophage tail fiber protein, participating in the initial steps of bacteriophage interaction with the bacterial host (Hsieh et al., 2017; Lin et al., 2017). Predictions of the TSP domain structure by AlphaFold 2 reveal three regions: N-terminal, central pyramid, and C-terminal, consistent with recently reported depolymerase structures derived from A. baumannii bacteriophages Drobiazko et al., 2022). After the expression and purification of 31TSP, it was discovered that the host range of depolymerase is wider than that of phage 31Y. Sensitive host of phage 31Y is limited to five strains of A. pittii, but sensitive host of 31TSP includes seven strains of A. pittii, one strain of A. nosocomialis, and 31 strains of A. baumannii. We also tested the sensitivity of some Gram-negative bacilli, such as Pseudomonas aeruginosa, Klebsiellas pneumoniae, E. coli and Enterobacter hormaechei, but no sensitive strains were found. As

31TSP showed a wider host range than original phage, methods on the T7 phage research could be used to investigate the mechanisms underlying host range alteration in future studies (Avramucz et al., 2021., Holtzman et al., 2024).

According previous notion (Chen et al., 2022; Liu et al., 2019a; Lin et al., 2017), the depolymerases generally do not directly kill bacteria during antibacterial therapy. But in this study, according to viable cell counting on bacteria treated with 31TSP, it was found that the number of bacteria in the depolymerase-treated group was significantly lower than that in the untreated group (Figure 3C). Furthermore, it has been demonstrated in many phage depolymerases exert their antibacterial effects in a trimeric form. For example, in Acinetobacter, the depolymerase Dpo71 from an A. baumannii phage exerts its antibacterial activity as a trimer (Abdelkader et al., 2022). However, in recent years, studies have also confirmed that some depolymerases exert their antibacterial function independently of trimer formation, such as the depolymerase from Klebsiella pneumoniae phage KP34 and the depolymerase that degrades the K2 serotype capsular polysaccharide of K. pneumoniae (Maciejewska et al., 2023; Ye et al., 2024). In this study, the structure of 31TSP was not verified by size

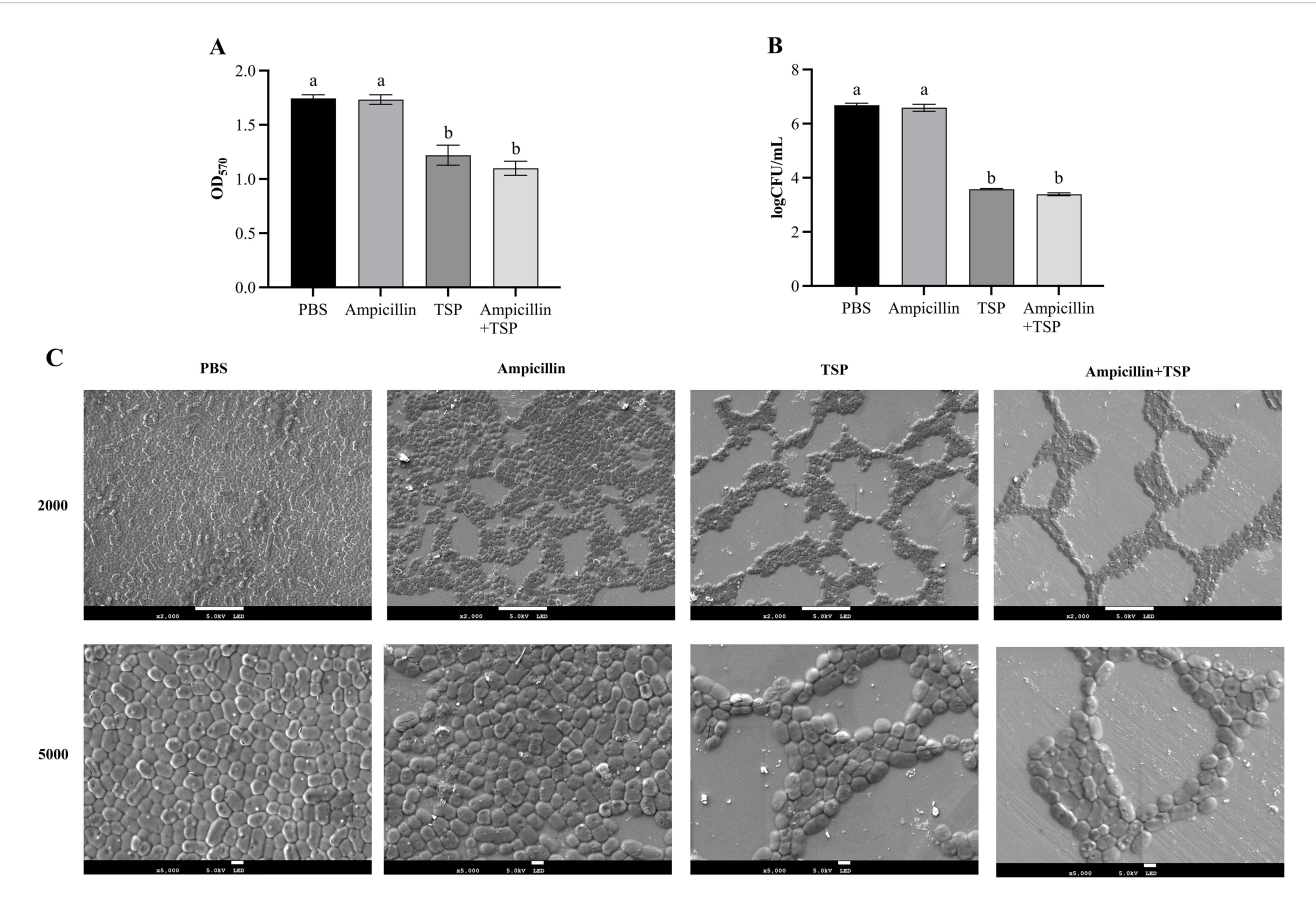


FIGURE 8
Disruption of Pre-formed Biofilms by 31TSP and Ampicillin. (A) Crystal violet staining. (B) Ap31 counting assay. (C) Scanning electron microscopy observation. Ap31 biofilms were initially cultured for 9 hours, followed by treatment with PBS (control), 31TSP (100 μ g/mL), ampicillin (16 μ g/mL, MIC), or their combination (31TSP + ampicillin) for 3 hours. Subsequently, crystal violet staining, bacterial counting, and scanning electron microscopy observation were performed. Data are presented as mean \pm SD (n = 3), and statistical analysis was conducted using one-way ANOVA. Groups sharing the same letter are not significantly different, while groups with different letters are significantly different (p < 0.05).

exclusion chromatography or circular dichroism analysis as in research of Dpo71. However, when we subjected the nickel-column purified depolymerase to low-temperature ultrafiltration using filters of different molecular weight cut-offs (MWCOs), we found that not only the flow-through fraction from the >100 kDa filter retained the ability to inhibit the growth of susceptible bacteria, but the <100 kDa fraction also contained material capable of inhibiting susceptible bacterial growth. Notably, the monomeric molecular weight of 31TSP is approximately 70 kDa. Therefore, further investigation is warranted regarding whether 31TSP's antibacterial function is dependent on trimer formation.

31TSP demonstrates remarkable stability in a wide range of physicochemical conditions, maintaining its activity between temperatures of 4°C to 121°C and within a pH range of 5-11. This impressive tolerance to extreme conditions suggests a correlation with the structural properties of bacteriophage depolymerases. These enzymes have evolved to endure harsh external environments during the course of evolution, ensuring the infectivity of bacteriophages (Oliveira et al., 2019). The observed heat resistance of 31TSP, even after exposure to high-pressure

treatment at 121°C for 30 minutes, appears to be reported for the first time. The stability of 31TSP across such a broad range of temperatures and pH levels makes it particularly promising for use in clinical settings or food industry.

In previous research, depolymerase contributing to enhanced susceptibility of bacteria to serum complement-mediated killing (Liu et al., 2020; Majkowska-Skrobek et al., 2018). However, in our serum bactericidal assay, target bacteria showed resistant to serum killing. In 31TSP sensitive strains, serum or inactivated serum even showed slightly inhibit effects to TSP (Figure 6). The reasons for this difference lie in the mechanism of action of TSP, a mechanism that remains elusive to date (Chen et al., 2022). Further studies are needed to elucidate the exact molecular mechanisms behind 31TSP's activity, as this could provide deeper insights into its clinical potential.

The formation of biofilms is a major factor contributing to the chronicity of bacterial infections and the increased antibiotic resistance (Sharma et al., 2019; Costerton et al., 1999). Depolymerases have proven valuable in inhibiting and/or eradicating biofilms formed by *Klebsiella* (Li et al., 2022; Wu et

al., 2019), Shiga toxin-producing *Escherichia coli* (Chen et al., 2020), and *A. baumannii* (Shahed-Al-Mahmud et al., 2021). The persistence and antibiotic resistance of *A. pittii* infections are strongly associated with biofilm formation. 31TSP demonstrates dual antibiofilm activity, exhibiting both preventive effects on biofilm formation and disruptive effects to mature biofilm. These properties suggest its potential as an adjunctive therapeutic agent to enhance the effectiveness of conventional antibiotics against biofilm-associated infections.

In this study, 31TSP alone demonstrated significant antibiofilm activity, effectively preventing biofilm formation and disrupting mature biofilms. We also tested the combination of 31TSP and ampicillin, which showed enhanced biofilm inhibition during prolonged treatment (24 h), but no significant improvement over 31TSP monotherapy was observed in disrupting pre-formed biofilms. As the ampicillin is not the first choice for treatment for clinical *Acinetobacter* infections, the combination test should choose carbapenem as test antibiotics, but all strains sensitive to 31TSP in our lab are also sensitive to carbapenem. Notably, beyond its activity against *A. pittii*, 31TSP demonstrated cross-species inhibitory effects against clinically isolated *A. nosocomialis* and *A. baumannii* strains. This broad host range not only enhances its potential clinical applicability but also provides valuable insights for future investigations into its host recognition mechanisms.

5 Conclusion

The depolymerase 31TSP demonstrates a broad host range to *A. pittii*, *A. baumannii*, and *A. nosocomialis*, maintaining functional stability across extensive pH (5–11) and temperature (4–121 °C) ranges. As a safe and effective antimicrobial agent, 31TSP exhibits dual functionality: (1) enzymatic degradation of bacterial capsular polysaccharides (CPS) and (2) direct bactericidal activity. While 31TSP alone significantly inhibits biofilm formation and disrupts mature biofilms (p < 0.05), its combination with ampicillin shows synergistic enhancement in biofilm prevention during prolonged exposure (24 h). These findings position phage-derived depolymerases, particularly 31TSP, as promising therapeutic candidates for combating *Acinetobacter* infections, especially in biofilm-associated cases.

Data availability statement

The datasets presented in this study can be found in online repositories. The names of the repository/repositories and accession number(s) can be found in the article/Supplementary Material.

Ethics statement

The bacterial strains used in this work did not involve any endangered or protected species, and did not require any specific permit or ethical approval in accordance with the local legislation and institutional requirements. All laboratory work was conducted following standard microbiological safety protocols. For the serum bactericidal assay using samples from a healthy laboratory volunteer, written informed consent was not required as the use of anonymized, voluntarily donated samples posed minimal risk and complied with institutional ethical guidelines.

Author contributions

NZ: Validation, Resources, Project administration, Formal analysis, Data curation, Conceptualization, Methodology, Visualization, Writing - review & editing, Investigation, Writing original draft, Software. WL: Project administration, Formal analysis, Writing - review & editing, Writing - original draft, Methodology, Data curation, Software, Conceptualization, Resources, Investigation, Visualization, Validation. XD: Methodology, Conceptualization, Software, Investigation, Writing - review & editing. DD: Methodology, Writing - review & editing, Visualization, Conceptualization, Investigation. M-AF: Methodology, Investigation, Writing - review & editing, Software. JX: Formal analysis, Writing - review & editing, Methodology. ZY: Investigation, Methodology, Writing - review & editing, Resources, Conceptualization. HJ: Data curation, Conceptualization, Resources, Formal analysis, Writing - review & editing. MS: Methodology, Writing - review & editing, Investigation. HH: Conceptualization, Visualization, Funding acquisition, Resources, Writing - review & editing, Formal analysis, Project administration, Supervision. SB: Resources, Writing - review & editing, Investigation, Formal analysis. HS: Writing - review & editing, Supervision, Conceptualization, Project administration, Resources.

Funding

The author(s) declare that no financial support was received for the research and/or publication of this article.

Conflict of interest

The authors declare that the research was conducted in the absence of any commercial or financial relationships that could be construed as a potential conflict of interest.

Generative Al statement

The author(s) declare that no Generative AI was used in the creation of this manuscript.

Any alternative text (alt text) provided alongside figures in this article has been generated by Frontiers with the support of artificial intelligence and reasonable efforts have been made to ensure accuracy, including review by the authors wherever possible. If you identify any issues, please contact us.

Publisher's note

All claims expressed in this article are solely those of the authors and do not necessarily represent those of their affiliated organizations, or those of the publisher, the editors and the reviewers. Any product that may be evaluated in this article, or claim that may be made by its manufacturer, is not guaranteed or endorsed by the publisher.

Supplementary material

The Supplementary Material for this article can be found online at: https://www.frontiersin.org/articles/10.3389/fcimb.2025. 1608526/full#supplementary-material

References

Abdelkader, K., Gutiérrez, D., Latka, A., Boeckaerts, D., Drulis-Kawa, Z., Criel, B., et al. (2022). The specific capsule depolymerase of phage PMK34 sensitizes acinetobacter baumannii to serum killing. Antibiotics (Basel). 11, 677. doi: 10.3390/antibiotics11050677

Avramucz, Á., Møller-Olsen, C., Grigonyte, A. M., Paramalingam, Y., Millard, A., Sagona, A. P., et al. (2021). Analysing parallel strategies to alter the host specificity of bacteriophage T7. *Biol. (Basel)*. 10, 556. doi: 10.3390/biology10060556

Bogaerts, P., Huang, T. D., Rezende de Castro, R., Bouchahrouf, W., and Glupczynski, Y. (2013). Could *Acinetobacter pittii* act as an NDM-1 reservoir for Enterobacteriaceae? *J. Antimicrob. Chemother.* 68, 2414–2415. doi: 10.1093/jac/dkt201

Cai, R. P., Gu, J. M., and Han, W. Y. (2020). Advances in research on classification, structural characteristics and applications of bacteriophage depolymerase. *Chin. J. Vet. Sci.* 40, 1258–1264.

Chen, F. J., Huang, W. C., Liao, Y. C., Wang, H. Y., Lai, J. F., Kuo, S. C., et al. (2019). Molecular Epidemiology of Emerging Carbapenem Resistance in *Acinetobacter nosocomialis* and *Acinetobacter pittii* in Taiwan 2010 to 2014. *Antimicrob. Agents Chemother.* 63, e02007–e02018. doi: 10.1128/AAC.02007-18

Chen, Y., Li, X., Wang, S., Guan, L., Li, X., Hu, D., et al. (2020). A novel tail-associated O91-specific polysaccharide depolymerase from a podophage reveals lytic efficacy of shiga toxin-producing *escherichia coli*. *Appl. Environ. Microbiol*. 86, e00145–e00120. doi: 10.1128/AEM.00145-20

Chen, X., Liu, M., Zhang, P., Xu, M., Yuan, W., Bian, L., et al. (2022). Phage-derived depolymerase as an antibiotic adjuvant against multidrug-resistant *acinetobacter baumannii*. Front. Microbiol. 13. doi: 10.3389/fmicb.2022.845500

Chen, L., Yuan, J., Xu, Y., Zhang, F., and Chen, Z. (2018). Comparison of clinical manifestations and antibiotic resistances among three genospecies of the *Acinetobacter calcoaceticus-Acinetobacter baumannii complex*. *PloS One* 13, e0191748. doi: 10.1371/journal.pone.0191748

Chusri, S., Chongsuvivatwong, V., Rivera, J. I., Silpapojakul, K., Singkhamanan, K., McNeil, E., et al. (2014). Clinical outcomes of hospital-acquired infection with Acinetobacter nosocomialis and Acinetobacter pittii. Antimicrob. Agents Chemother. 58, 4172–4179. doi: 10.1128/AAC.02992-14

Cosgaya, C., Ratia, C., Marí-Almirall, M., Rubio, L., Higgins, P. G., Seifert, H., et al. (2019). *In vitro* and *in vivo* Virulence Potential of the Emergent Species of the *Acinetobacter baumannii* (Ab) Group. *Front. Microbiol.* 10. doi: 10.3389/fmicb.2019.02429

Costerton, J. W., Stewart, P. S., and Greenberg, E. P. (1999). Bacterial biofilms: a common cause of persistent infections. *Science* 284, 1318–1322. doi: 10.1126/science.284.5418.1318

Cui, X., Du, B., Feng, J., Feng, Y., Fan, Z., Chen, J., et al. (2023). A novel phage carrying capsule depolymerase effectively relieves pneumonia caused by multidrug-resistant Klebsiella aerogenes. *J. BioMed. Sci.* 30, 75. doi: 10.1186/s12929-023-00946-y

Domingues, R., Barbosa, A., Santos, S. B., Pires, D. P., Save, J., Resch, G., et al. (2021). Unpuzzling Friunavirus-Host Interactions One Piece at a Time: Phage Recognizes Acinetobacter pittii via a New K38 Capsule Depolymerase. *Antibiotics* 10, 1304. doi: 10.3390/antibiotics10111304

Drobiazko, A. Y., Kasimova, A. A., Evseev, P. V., Shneider, M. M., Klimuk, E. I., Shashkov, A. S., et al. (2022). Capsule-targeting depolymerases derived from *acinetobacter baumannii* prophage regions. *Int. J. Mol. Sci.* 23, 4971. doi: 10.3390/ijms23094971

Garcia-Doval, C., and van Raaij, M. J. (2012). Structure of the receptor-binding carboxy-terminal domain of bacteriophage T7 tail fibers. *Proc. Natl. Acad. Sci. U S A.* 109, 9390–9395. doi: 10.1073/pnas.1119719109

Holtzman, T., Nechooshtan, R., Yosef, I., and Qimron, U. (2024). Contracting the host range of bacteriophage T7 using a continuous evolution system. *Methods Mol. Biol.* 2793, 85–100. doi: 10.1007/978-1-0716-3798-2_6

Hsieh, P. F., Lin, H. H., Lin, T. L., Chen, Y. Y., and Wang, J. T. (2017). Two T7-like bacteriophages, K5–2 and K5-4, each encodes two capsule depolymerases: isolation and functional characterization. *Sci. Rep.* 7, 4624. doi: 10.1038/s41598-017-04644-2

Iimura, M., Hayashi, W., Arai, E., Natori, T., Horiuchi, K., Matsumoto, G., et al. (2020). Detection of *Acinetobacter pittii* ST220 co-producing NDM-1 and OXA-820 carbapenemases from a hospital sink in a non-endemic country of NDM. *J. Glob Antimicrob. Resist.* 21, 353–356. doi: 10.1016/j.jgar.2019.11.013

Jumper, J., Evans, R., Pritzel, A., Green, T., Figurnov, M., Ronneberger, O., et al. (2021). Highly accurate protein structure prediction with AlphaFold. *Nature* 596, 583–589. doi: 10.1038/s41586-021-03819-2

Kiyasu, Y., Hitomi, S., Funayama, Y., Saito, K., and Ishikawa, H. (2020). Characteristics of invasive *Acinetobacter* infection: A multicenter investigation with molecular identification of causative organisms. *J. Infect. Chemother.* 26, 475–482. doi: 10.1016/j.jiac.2019.12.010

Kropinski, A. M., Mazzocco, A., Waddell, T. E., Lingohr, E., and Johnson, R. P. (2009). Enumeration of bacteriophages by double agar overlay plaque assay. *Methods Mol. Biol.* 501, 69–76. doi: 10.1007/978-1-60327-164-6_7

Kuo, S. C., Lee, Y. T., Yang, S. P., Chiang, M. C., Lin, Y. T., Tseng, F. C., et al. (2013). Evaluation of the effect of appropriate antimicrobial therapy on mortality associated with Acinetobacter nosocomialis bacteraemia. *Clin. Microbiol. Infect.* 19, 634–639. doi: 10.1111/j.1469-0691.2012.03967.x

La Scola, B., Gundi, V. A., Khamis, A., and Raoult, D. (2006). Sequencing of the rpoB gene and flanking spacers for molecular identification of *Acinetobacter species. J. Clin. Microbiol.* 44, 827–832. doi: 10.1128/JCM.44.3.827-832.2006

Li, J., Sheng, Y., Ma, R., Xu, M., Liu, F., Qin, R., et al. (2021). Identification of a depolymerase specific for K64-serotype *klebsiella pneumoniae*: potential applications in capsular typing and treatment. *Antibiotics (Basel)*. 10, 144. doi: 10.3390/antibiotics10020144

Lee, Y. T., Sun, J. R., Wang, Y. C., Chiu, C. H., Kuo, S. C., Chen, T. L., et al. (2021) Corrigendum to "Multicentre study of risk factors for mortality in patients with Acinetobacter bacteraemia receiving colistin treatment". *Int J Antimicrob Agents*. 57, 106333. doi: 10.1016/j.ijantimicag.2021.106333

Li, M., Wang, H., Chen, L., Guo, G., Li, P., Ma, J., et al. (2022). Identification of a phage-derived depolymerase specific for KL47 capsule of *Klebsiella pneumoniae* and its therapeutic potential in mice. *Virol. Sin.* 37, 538–546. doi: 10.1016/j.virs.2022.04.005

Lin, H., Paff, M. L., Molineux, I. J., and Bull, J. J. (2017). Therapeutic Application of Phage Capsule Depolymerases against K1, K5, and K30 Capsulated *E. coli* in Mice. *Front. Microbiol.* 8. doi: 10.3389/fmicb.2017.02257

Liu, Y. M., Lee, Y. T., Kuo, S. C., Chen, T. L., Liu, C. P., and Liu, C. E. (2017). Comparison between bacteremia caused by Acinetobacter pittii and Acinetobacter nosocomialis. *J. Microbiol. Immunol. Infect.* 50, 62–67. doi: 10.1016/j.jmii.2015.01.003

Liu, Y., Leung, S. S. Y., Guo, Y., Zhao, L., Jiang, N., Mi, L., et al. (2019a). The Capsule Depolymerase Dpo48 Rescues *Galleria mellonella* and Mice From *Acinetobacter baumannii* Systemic Infections. *Front. Microbiol.* 10. doi: 10.3389/fmicb.2019.00545

Liu, Y., Leung, S. S. Y., Huang, Y., Guo, Y., Jiang, N., Li, P., et al. (2020). Identification of two depolymerases from phage IME205 and their antivirulent functions on K47 capsule of *klebsiella pneumoniae*. *Front. Microbiol.* 11. doi: 10.3389/fmicb.2020.00218

Liu, Y., Mi, Z., Mi, L., Huang, Y., Li, P., Liu, H., et al. (2019b). Identification and characterization of capsule depolymerase Dpo48 from *Acinetobacter baumannii* phage IME200. *PeerJ* 7, e6173. doi: 10.7717/peerj.6173

Lu, S., Le, S., Tan, Y., Zhu, J., Li, M., Rao, X., et al. (2013). Genomic and proteomic analyses of the terminally redundant genome of the *Pseudomonas aeruginosa* phage PaP1: establishment of genus PaP1-like phages. *PloS One* 8, e62933. doi: 10.1371/journal.pone.0062933

Luong, T., Salabarria, A. C., Edwards, R. A., and Roach, D. R. (2020). Standardized bacteriophage purification for personalized phage therapy. *Nat. Protoc.* 15, 2867–2890. doi: 10.1038/s41596-020-0346-0

Maciejewska, B., Squeglia, F., Latka, A., Privitera, M., Olejniczak, S., Switala, P., et al. (2023). *Klebsiella* phage KP34gp57 capsular depolymerase structure and function: from a serendipitous finding to the design of active mini-enzymes against K. pneumoniae. *mBio* 14, e0132923. doi: 10.1128/mbio.01329-23

Majkowska-Skrobek, G., Latka, A., Berisio, R., Squeglia, F., Maciejewska, B., Briers, Y., et al. (2018). Phage-borne depolymerases decrease *klebsiella pneumoniae* resistance to innate defense mechanisms. *Front. Microbiol.* 9. doi: 10.3389/fmicb.2018.02517

Marí-Almirall, M., Cosgaya, C., Pons, M. J., Nemec, A., Ochoa, T. J., Ruiz, J., et al. (2019). Pathogenic Acinetobacter species including the novel *Acinetobacter dijkshoorniae* recovered from market meat in Peru. *Int. J. Food Microbiol.* 305, 108248. doi: 10.1016/j.ijfoodmicro.2019.108248

Molina, J., Cisneros, J. M., Fernández-Cuenca, F., Rodríguez-Baño, J., Ribera, A., Beceiro, A., et al. (2010). Clinical features of infections and colonization by Acinetobacter genospecies 3. *J. Clin. Microbiol.* 48, 4623–4626. doi: 10.1128/JCM.01216-10

Oliveira, H., Costa, A. R., Ferreira, A., Konstantinides, N., Santos, S. B., Boon, M., et al. (2019). Functional analysis and antivirulence properties of a new depolymerase from a myovirus that infects *acinetobacter baumannii* capsule K45. *J. Virol.* 93, e01163–e01118. doi: 10.1128/JVI.01163-18

Oliveira, H., Costa, A. R., Konstantinides, N., Ferreira, A., Akturk, E., Sillankorva, S., et al. (2021). Ability of phages to infect Acinetobacter calcoaceticus-Acinetobacter baumannii complex species through acquisition of different pectate lyase depolymerase domains. *Environ. Microbiol.* 23, 3334. doi: 10.1111/1462-2920.15620

Paczosa, M. K., and Mecsas, J. (2016). *Klebsiella pneumoniae*: going on the offense with a strong defense. *Microbiol. Mol. Biol. Rev.* 80, 629–661. doi: 10.1128/MMBR.00078-15

Pailhoriès, H., Hadjadj, L., Mahieu, R., Crochette, N., Rolain, J. M., and Kempf, M. (2017). Fortuitous diagnosis of NDM-1-producing Acinetobacter pittii carriage in a patient from France with no recent history of travel. *J. Antimicrob. Chemother.* 72, 942–944. doi: 10.1093/jac/dkw505

Pailhoriès, H., Tiry, C., Eveillard, M., and Kempf, M. (2018). *Acinetobacter pittii* isolated more frequently than Acinetobacter baumannii in blood cultures: the experience of a French hospital. *J. Hosp Infect.* 99, 360–363. doi: 10.1016/j.jhin.2018.03.019

Pires, D. P., Oliveira, H., Melo, L. D., Sillankorva, S., and Azeredo, J. (2016). Bacteriophage-encoded depolymerases: their diversity and biotechnological applications. *Appl. Microbiol. Biotechnol.* 100, 2141–2151. doi: 10.1007/s00253-015-7247-0

Rice, C. J., Kelly, S. A., O'Brien, S. C., Melaugh, E. M., Ganacias, J. C. B., Chai, Z. H., et al. (2021). Novel Phage-Derived Depolymerase with Activity against *Proteus mirabilis* Biofilms. *Microorganisms* 9, 2172. doi: 10.3390/microorganisms9102172

Ringaci, A., Shevchenko, K. G., Zelepukin, I. V., Popova, A. V., and Nikitin, M. P. (2022). Phage-mimicking nanoagents for rapid depolymerase specificity screening against multidrug resistant bacteria. *Biosens Bioelectron.* 213, 114444. doi: 10.1016/j.bios.2022.114444

Shahed-Al-Mahmud, M., Roy, R., Sugiokto, F. G., Islam, M. N., Lin, M. D., Lin, L. C., et al. (2021). Phage φAB6-borne depolymerase combats acinetobacter baumannii biofilm formation and infection. Antibiotics (Basel). 10, 279. doi: 10.3390/antibiotics1030279

Sharma, D., Misba, L., and Khan, A. U. (2019). Antibiotics versus biofilm: an emerging battleground in microbial communities. *Antimicrob. Resist. Infect. Control.* 8, 76. doi: 10.1186/s13756-019-0533-3

Söding, J., Biegert, A., and Lupas, A. N. (2005). The HHpred interactive server for protein homology detection and structure prediction. *Nucleic Acids Res.* 33, W244–W248. doi: 10.1093/nar/gki408

Teixeira, A. B., Barin, J., Hermes, D. M., Barth, A. L., and Martins, A. F. (2017). PCR Assay Based on the gyrB Gene for Rapid Identification of *Acinetobacter baumannii-calcoaceticus* Complex at Specie Level. *J. Clin. Lab. Anal.* 31, e22046. doi: 10.1002/jcla.22046

Tian, C., Xing, M., Fu, L., Zhao, Y., Fan, X., and Wang, S. (2022). Emergence of uncommon KL38-OCL6-ST220 carbapenem-resistant *Acinetobacter pittii* strain, coproducing chromosomal NDM-1 and OXA-820 carbapenemases. *Front. Cell Infect. Microbiol.* 12. doi: 10.3389/fcimb.2022.943735

Vijayakumar, S., Biswas, I., and Veeraraghavan, B. (2019). Accurate identification of clinically important Acinetobacter spp.: an update. *Future Sci. OA.* 5, FSO395. doi: 10.2144/fsoa-2018-0127

Walmagh, M., Boczkowska, B., Grymonprez, B., Briers, Y., Drulis-Kawa, Z., and Lavigne, R. (2013). Characterization of five novel endolysins from Gram-negative infecting bacteriophages. *Appl. Microbiol. Biotechnol.* 97, 4369–4375. doi: 10.1007/s00253-012-4294-7

Wilson, C., Lukowicz, R., Merchant, S., Valquier-Flynn, H., Caballero, J., Sandoval, J., et al. (2017). Quantitative and qualitative assessment methods for biofilm growth: A mini-review. Res. Rev. J. Eng. Technol. 6. Available online at: http://www.rroij.com/open-access/quantitative-and-qualitative-assessment-methods-for-biofilm-growth-a-minireview-.pdf.

Wu, Y., Wang, R., Xu, M., Liu, Y., Zhu, X., Qiu, J., et al. (2019). A Novel Polysaccharide Depolymerase Encoded by the Phage SH-KP152226 Confers Specific Activity Against Multidrug-Resistant *Klebsiella pneumoniae* via Biofilm Degradation. *Front. Microbiol.* 10. doi: 10.3389/fmicb.2019.02768

Yang, L., Dong, N., Xu, C., Ye, L., and Chen, S. (2021). Emergence of ST63 pandrug-resistant *acinetobacter pittii* isolated from an AECOPD patient in China. *Front. Cell Infect. Microbiol.* 11. doi: 10.3389/fcimb.2021.739211

Ye, T. J., Fung, K. M., Lee, I. M., Ko, T. P., Lin, C. Y., Wong, C. L., et al. (2024). *Klebsiella pneumoniae* K2 capsular polysaccharide degradation by a bacteriophage depolymerase does not require trimer formation. *mBio* 15, e03519-23

Yuan, Y., Li, X., Wang, L., Li, G., Cong, C., Li, R., et al. (2021). The endolysin of the *Acinetobacter baumannii* phage vB_AbaP_D2 shows broad antibacterial activity. *Microb. Biotechnol.* 14, 403–418. doi: 10.1111/1751-7915.13594

Zhu, R., and Mathur, V. (2022). Prophages present in *acinetobacter pittii* influence bacterial virulence, antibiotic resistance, and genomic rearrangements. *Phage (New Rochelle)*. 3, 38–49. doi: 10.1089/phage.2021.0014